The Astronomical Journal, 138:1072–1081, 2009 October doi:10.1088/0004-6256/138/4/1072

HERBIG–HARO OBJECTS IN THE LUPUS I AND III MOLECULAR CLOUDS

Hongchi Wang[1] and Thomas Henning[2]
[1] Purple Mountain Observatory, Chinese Academy of Sciences, Nanjing 210008, China; hcwang@pmo.ac.cn
[2] Max-Planck-Institut für Astronomie, Königstuhl 17, D-69117 Heidelberg, Germany
Received 2008 December 1; accepted 2009 August 1; published 2009 September 1

ABSTRACT

We performed a deep search for Herbig–Haro (HH) objects toward the Lupus I and III clouds, covering a sky area of ~ 1 and ~ 0.5 deg^2, respectively. In total, 11 new HH objects, HH 981–991, are discovered. The HH objects both in Lupus I and in Lupus III tend to be concentrated in small areas. The HH objects detected in Lupus I are located in a region of radius 0.26 pc near the young star Sz 68. The abundance of HH objects shows that this region of the cloud is active in on-going star formation. HH objects in the Lup III cloud are concentrated in the central part of the cloud around the Herbig Ae/Be stars HR 5999 and 6000. HH 981 and 982 in Lupus I are probably driven by the young brown dwarf SSTc2d J154457.9−342340 which has a mass of 50 M_J. HH 990 and 991 in Lup III align well with the HH 600 jet emanating from the low-mass star Par-Lup3-4, and are probably excited by this low-mass star of spectral type M5. High proper motions for HH 228 W, E, and E2 are measured, which confirms that they are excited by the young star Th 28. In contrast, HH 78 exhibits no measurable proper motion in the time span of 18 years, indicating that HH 78 is unlikely part of the HH 228 flow. The HH objects in Lup I and III are generally weak in terms of brightness and dimension in comparison to HH objects we detected with the same technique in the R CrA and Cha I clouds. Through a comparison with the survey results from the *Spitzer* c2d program, we find that our optical survey is more sensitive, in terms of detection rate, than the *Spitzer* IRAC survey to high-velocity outflows in the Lup I and III clouds.

Key words: ISM: Herbig–Haro objects – ISM: individual (Lupus I and III) – ISM: jets and outflows – stars: formation

1. INTRODUCTION

Outflows from young stars are found to be ubiquitous at the early stages of star formation and have been observed in various wavelengths from X-ray, UV, optical, infrared, millimeter to radio wavelengths (see, e.g., Bally et al. 2007; Arce et al. 2007). Observations at different wavelengths trace different components of the outflows. For example, Herbig–Haro (HH) objects observed in the visual (for a review on HH objects, see, e.g., Reipurth & Bally 2001) trace shocked ionized gas with temperature around 10^4 K and CO molecular outflows observed at millimeter wavelengths (for a review on CO molecular outflows, see, e.g., Bachiller 1996) trace molecular gas entrained by high-velocity jets which usually has a temperature of a few tens Kelvin. As shocked regions, HH objects have characteristic optical spectra that exhibit strong forbidden lines such as [O I] λλ 6300/6363, [N II] λλ 6548/6584, and [S II] λλ 6717/6731 (Solf et al. 1988; Hartigan et al. 1999). The spectra of HH objects differ from those of the photo-ionized regions, such a planetary nebula and H II regions, in that these nebulae usually have much weaker low-excitation lines, such as [S II] λλ 6717/6731 (Kwitter & Henry 1998; Osterbrock et al. 1992). Supernova remnants have similar optical spectra as HH objects (Fesen & Hurford 1996). These nebulae, however, have much larger sizes than HH objects and are rarely located in star-forming regions. Therefore, imaging with a narrowband filter covering the [S II] λλ 6717/6731 lines and a neighboring slightly blue- or redshifted filter or a red broadband filter that avoids the strong lines of HH objects has proven to be an effective and efficient technique in identifying HH objects in star-forming regions (Reipurth & Graham 1988; Yan et al. 1998; Wang et al. 2004; Walawender et al. 2005).

The dynamical ages of HH objects are relatively short, lying in the range of 10^3–10^5 yr, which makes HH objects a good tracer of recent star formation. Outflows from young stellar objects (YSOs) are generally believed to be driven by mass accretion from circumstellar disks onto the central stars (Shang et al. 2007; Pudritz et al. 2007). Therefore, observations of outflow phenomena can impose strong constraints on the formation mechanisms of their driving sources. For example, spectroscopic signatures of outflows from young brown dwarfs have been found in several cases (Fernández & Comerón 2001; Barrado y Navascués et al. 2004; Natta et al. 2004; Whelan et al. 2005), which provides support to the core-collapse scenario of brown dwarf formation (Whitworth et al. 2007). However, direct imaging evidence for a brown dwarf to drive an outflow is still lacking. Taking advantage of the large field of view provided by mosaic CCDs and using HH objects as a tracer of recent star formation, we have conducted a campaign to investigate the star formation activity in nearby star-forming regions with an emphasis on the search for outflows from very low-mass stars and brown dwarfs. Our survey has covered the R CrA, Cha I, Lupus I and III star-forming regions. In this paper we report results from our survey of the Lupus I and III clouds. For our survey results on the R CrA and Cha I clouds, see Wang et al. (2004) and Wang & Henning (2006).

The Lupus molecular complex covers a wide area on the sky with a spatial extent of $\sim 20^\circ$. It consists of a number of dark clouds (Krautter 1991). Among them Lupus III is the most active region of star formation, associated with more than 40 T Tauri stars (Schwartz 1977) and the Herbig Ae/Be stars HR 5999 and HR 6000. The distance to the Lupus clouds is still controversial, ranging from 100 pc (Knude & Høg 1998) to 190 pc (Wichmann et al. 1998). Using extinction maps from the Two Micron All Sky Survey (2MASS) and parallaxes from Hipparcos and Tycho, Lombardi et al. (2008) obtained a distance of 155 ± 8 pc for the Lupus complex. For this study we use the conventional value of 150 pc (Krautter 1991). Molecular line

observations in ^{13}CO ($J = 1$–0) have shown that both Lupus I and III have a filamentary structure with a mass of $\sim 1200\ M_\odot$ and 300 $M_\odot$, respectively (Tachihara et al. 1996). ^{18}CO and H^{13}CO$^+$ dense cores have been observed in both clouds (Hara et al. 1999). Tachihara et al. (2007) detected an embedded millimeter-wave source in the Lupus III cloud, Lup 3 MMS, and identified it to be a Class 0 object. The Lupus III region has been surveyed for very low-mass stars and brown dwarfs in the visual and near-infrared wavelengths (Nakajima et al. 2000; Comerón et al. 2003; López Martí et al. 2005). Previously, Heyer & Graham (1989) found three HH objects, HH 185-187, in the Lupus I cloud, and Krautter (1986) and Reipurth & Graham (1988) discovered two HH objects, HH 78 and 228, in Lupus III. Recently, Fernández & Comerón (2005) discovered a jet emanating from the low-mass star Par-Lup3-4. This jet is later designated as HH 600 in Comerón (2008). The Lupus I and III clouds also have been imaged with the IRAC and the MIPS instruments of the *Spitzer Space Telescope* in the c2d program (Allen et al. 2007; Chapman et al. 2007; Merín et al. 2008). As a result, 141 YSOs have been identified in the Lupus I and III clouds based on their spectral energy distributions in the K-24 μm wavelength range. More details about the Lupus clouds can be found in Comerón (2008).

2. OBSERVATIONS AND DATA REDUCTION

The observations were made using the ESO/MPG 2.2 m telescope at La Silla. The Lupus III molecular cloud was observed on 2004 July 10–18 and the Lupus I molecular cloud was observed on 2005 April 4–10. The telescope is equipped with the Wide Field Imager (WFI) camera which is a mosaic of eight 2k × 4k CCDs with narrow interchip gaps (the filling factor is 95.9%; Baade 2002). With a plate scale of $0\farcs238$ pixel^{-1}, the total field of view of WFI is $34' \times 33'$. The combination of the filters ESO 857 and ESO 847 was used for the observations. The ESO 857 filter is a narrowband filter with a central wavelength of $\lambda_c = 6763.4$ Å and a bandpass of $\Delta\lambda = 84.2$ Å. Its transmission at the characteristic lines of HH objects, [S II] $\lambda\lambda$ 6717/6731, is 0.31 and 0.63, respectively. The ESO 847 filter, an intermediate-band filter with a central wavelength of $\lambda_c = 7217.9$ Å and a bandpass of $\Delta\lambda = 256.5$ Å, was used to measure the continuum emission. The obtained data were processed in the same way as in Wang et al. (2004) and Wang & Henning (2006).

Totally five fields toward the Lupus I cloud and two fields toward the Lupus III cloud were observed during our survey (see Figures 1 and 2). To eliminate the effects of interchip gaps, cosmic rays, and bad pixels, typically six frames were taken in each of the ESO 857 and ESO 847 filters with the telescope pointing being slightly offset. In the ESO 857 filter, both field 1 in Lupus I and in Lupus III (see Figures 1 and 2) were observed with 8 frames, and field 2 in Lupus I was observed with 14 frames. The exposures in the ESO 857 and ESO 847 filters for each frame were 1350 and 450 s, respectively. The seeing during the observations taken in 2004 July was around $1\farcs0$ and the seeing in the 2005 April observing run was around $1\farcs2$.

3. RESULTS AND DISCUSSION

With a total sky coverage of ~ 1 and ~ 0.5 deg^2 toward the Lupus I and III molecular clouds respectively, we have made a deep survey of these two nearby star-forming regions for HH objects. The five observed fields toward Lupus I and the two fields toward Lupus III, each with a field of view of $\sim 34' \times 33'$, are shown in Figures 1 and 2.

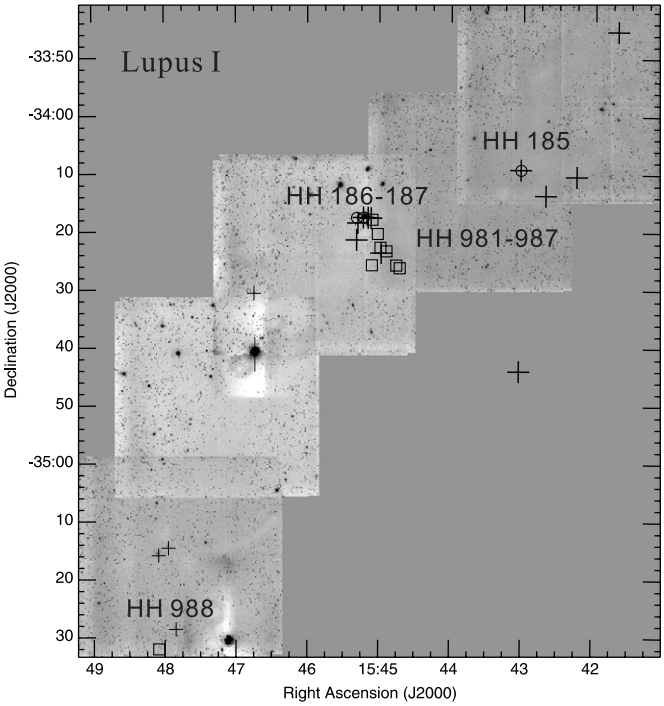

Figure 1. Mosaic [S II] image of the Lupus I cloud. The locations of newly detected HH objects, HH 981–988, are marked with squares. The three previously known HH objects in this region, HH 185–187 (Heyer & Graham 1989), are indicated with circles. The large pluses mark the locations of YSOs from Merín et al. (2008). The small pluses mark the locations of T Tauri stars from Herbig & Bell (1988) which are outside of the survey area of Merín et al. (2008). The observed fields 1–5 are from lower left to upper right.

Totally 17 HH objects are detected in our survey of the Lupus I and III clouds. Among the detections, 11 HH objects, i.e. HH 981–991, are newly found in our survey. The numbers for these newly detected HH objects are assigned by Bo Reipurth who is in charge of the numbering of HH objects on behalf of the IAU Nomenclature Committee. The distribution of HH objects in the Lupus I and III clouds is highly clustered. In the Lupus I cloud, 9 out of 11 HH objects detected in the cloud are located in a region of radius less than $6'$, a linear radius of 0.26 pc at the distance of 150 pc. All the HH objects found in the Lupus III cloud are concentrated in the central part of the cloud. The coordinates of the newly found HH objects are listed in Table 1. Using the transmittance of the broad *R*-band and the narrowband S II filters together with the zero point for the broad *R*-band filter, and assuming for simplicity that the [S II] λ 6717 flux is equal to the [S II] λ 6731 flux, we estimated that our detection limit of [S II] $\lambda\lambda$6717/6731 emission is 3.3×10^{-20} W m^{-2} arcsec^{-2} (3σ). Our images have a higher sensitivity and spatial resolution than previous observations of the Lupus I and III clouds, therefore, the coordinates for previously detected HH objects are listed in Table 2. High proper motions have been measured for the features W, E, and E2 in the HH 228 flow with W moving west and E and E2 east from Th 28, confirming that the HH 228 flow is powered by the T Tauri star Th 28. HH 78 exhibits nearly no measurable proper motion in a time span of 18 yr, which excludes the possibility that HH 78 is physically associated with the HH 228 flow. For other previously known HH objects in the Lupus I and III clouds, i.e., HH 185–187, only rough coordinates were reported in the literature (Heyer & Graham 1989), which excludes the possibility of making any meaningful determinations of proper motion for these objects.

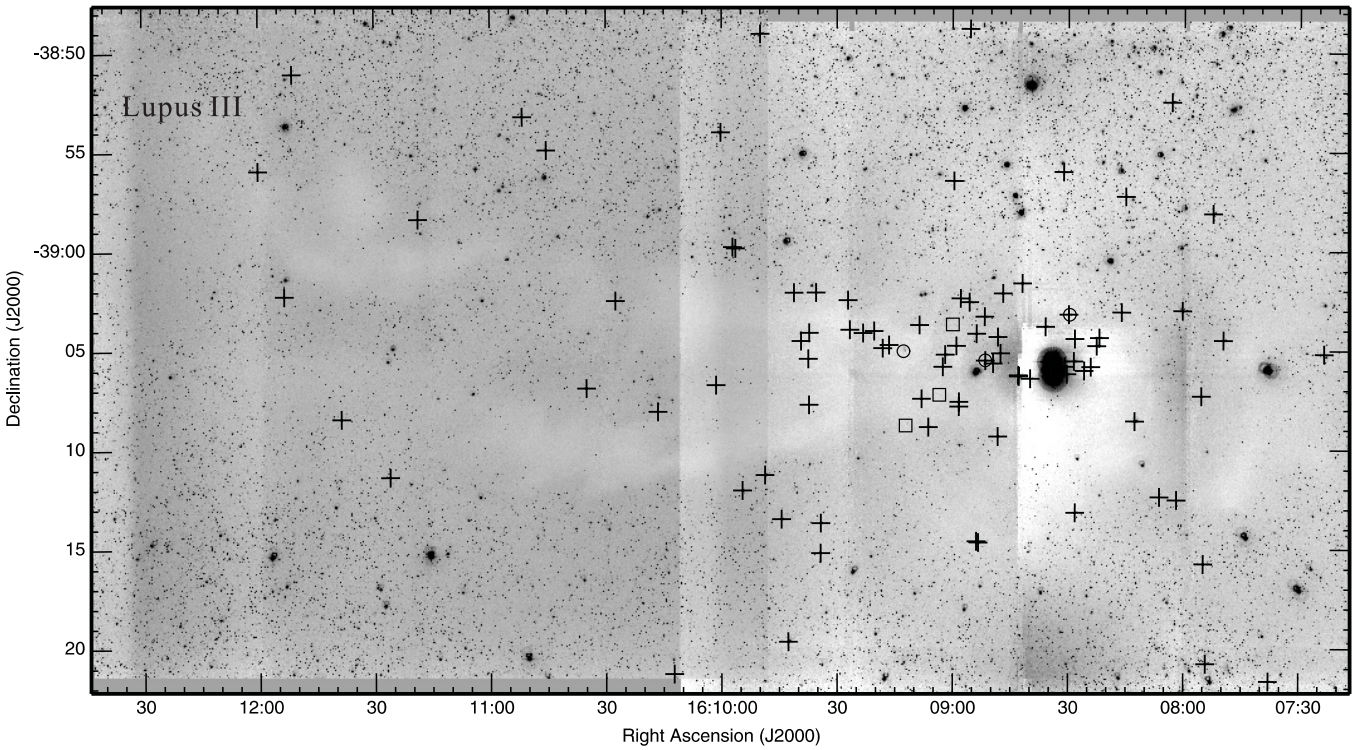

Figure 2. Mosaic [S II] image of the Lupus III cloud. The locations of newly detected HH objects, HH 989-991, are marked with squares. The locations of previously known HH objects, HH 78, 228, and 600 are marked with circles. Pluses mark the locations of YSOs from Merín et al. (2008). Observed fields 1–2 are from left to right.

Table 1
Newly Discovered Herbig–Haro Objects in Lup I and III

Object	α (J2000) (^{h} ^{m} ^{s})	δ (J2000) ($^{\circ}$ $'$ $''$)	Comments
HH 981...	15 44 42.7	−34 26 13	knot and diffuse patch
HH 982...	15 44 45.5	−34 25 46	bright knot with a long tail
HH 983 A...	15 44 53.8	−34 23 19	patch
HH 983 B...	15 44 53.6	−34 23 16	patch
HH 983 C...	15 44 53.8	−34 23 15	patch
HH 984 A...	15 44 58.9	−34 22 41	knot
HH 984 B...	15 44 59.2	−34 22 38	knot
HH 985...	15 45 01.1	−34 20 19	diffuse patch
HH 986...	15 45 05.6	−34 17 52	faint knot with a tail
HH 987...	15 45 05.9	−34 25 43	elongated knot with a tail
HH 988...	15 48 05.0	−35 32 03	faint patch
HH 989...	16 09 00.0	−39 03 41	faint patch
HH 990 A...	16 09 03.5	−39 07 14	elongated knot
HH 990 B...	16 09 04.1	−39 07 17	faint patch
HH 991...	16 09 12.2	−39 08 47	coma-shaped patch

Table 2
Previously Known Herbig–Haro Objects in Our Survey Area

Object	α (J2000) (^{h} ^{m} ^{s})	δ (J2000) ($^{\circ}$ $'$ $''$)	Comments
HH 185...	15 43 01.3	−34 09 16	patch with a central concentration
HH 186[a]...	15 45 12.9	−34 17 31	jet emanating from Sz 68
HH 187...	15 45 19.0	−34 17 33	knot
HH 228 W...	16 08 25.9	−39 03 06	elongated bright knot
HH 228[a]...	16 08 29.7	−39 03 11	jet emanating from Th 28
HH 228 E...	16 08 33.0	−39 03 17	faint patch
HH 228 E2...	16 08 37.9	−39 03 23	faint patch
HH 600[a]...	16 08 51.4	−39 05 30	short jet emanating from Par-Lup3-4
HH 78...	16 09 12.7	−39 05 03	elongated bright knot and diffuse patches

Notes.
[a] Coordinates in Columns 2 and 3 are for the position of the driving source.

To estimate the accuracy of our astrometry, we compared the coordinates of stars measured from our [S II] images with those compiled in the USNO2 catalog. It was found that our astrometry is accurate within 0.″3 both in R.A. and decl.

3.1. HH Objects in the Lupus I Cloud

Five fields, each with a field of view of $34' \times 33'$, are observed toward the Lupus I cloud. These fields cover most of the area of the Lupus I cloud (for CO maps of the Lupus cloud complex, see Tachihara et al. 2001). In total, 11 HH objects are detected in this region, including the previously known HH objects HH 185–187. Apart from HH 185 and the newly found HH 988, all the other HH objects found in this cloud are clustered in a region of radius less than $6'$ (see Figure 1). Previous studies have shown that the Lupus I cloud has only modest star formation activity (Krautter 1991). Our results of the HH object survey of this region confirm that this cloud is in general inactive in star formation. However, the Sz 68 region in the cloud hosts nine HH objects and two CTTSs, Sz 68 and 69 (Herbig & Bell 1988). Recently four new YSOs have been found in this region based on 2MASS and *Spitzer* observations (Allers et al. 2006; Chapman et al. 2007; Merín et al. 2008). These signatures of star formation indicate that this region of the Lupus I cloud has a high level of recent star formation.

The newly found HH objects HH 981–987 are located in the Sz 68 region of the Lupus I cloud (see Figure 3). HH 981 is located in the southwest of this region. It consists of a knot

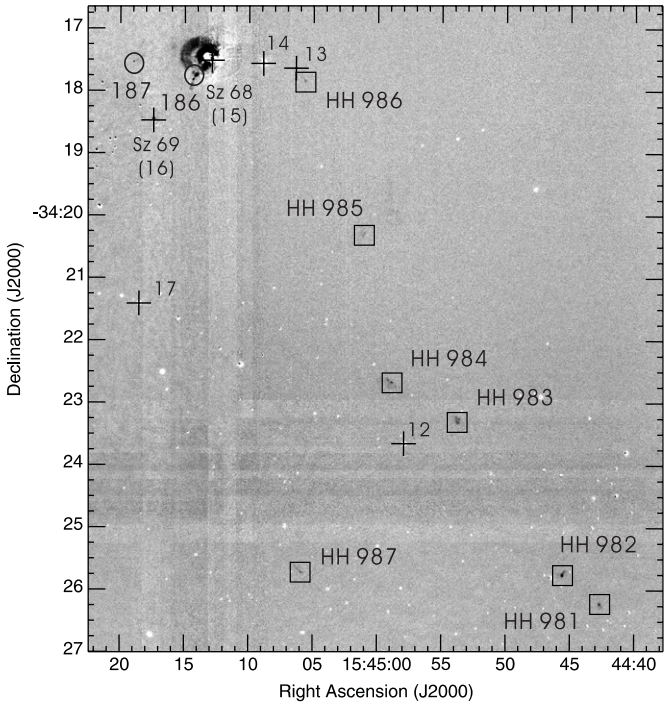

Figure 3. Continuum subtracted [S II] image of HH 981–987 in the Sz 68 region. The newly detected HH objects, HH 981–987, are indicated with squares. The previously known HH objects, HH 186 and 187, are indicated with circles. YSOs 12–17 from Merín et al. (2008) are marked with pluses. The object YSO 12 is a young brown dwarf (SSTc2d J154457.9−342340, see Allers et al. 2006) and is well aligned with HH 981 and 982.

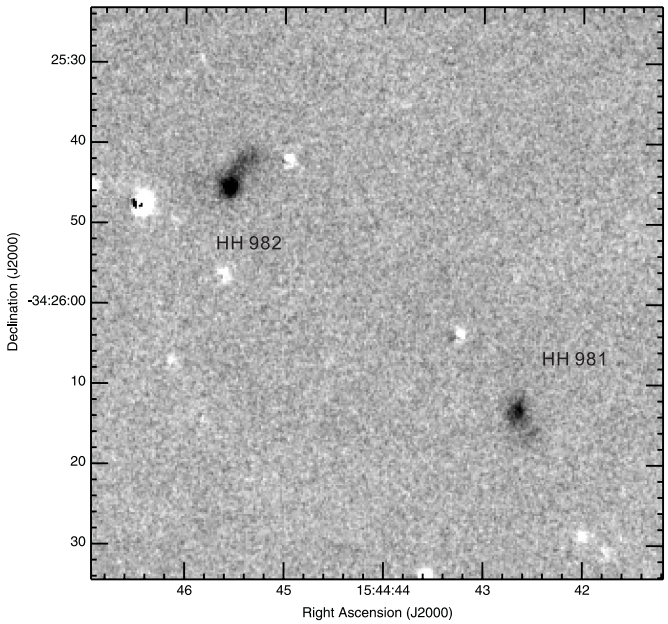

Figure 4. Continuum subtracted [S II] image of HH 981 and 982.

and diffuse emission to the southwest (see Figure 4). About 46″ to the northeast of HH 981 the source HH 982 is located (see Figure 4) which is a bright knot with a long tail extending to the northwest. From Figure 3 it can been seen that HH 981 and 982 align well with the nearby Class II YSO, SSTc2d J154457.9−342340 (YSO 12 in Table 5 of Merín et al. 2008). HH 981 and 982 probably represent an outflow driven by this source which is a young brown dwarf with a mass of 50 M_J (Allers et al. 2006). HH 983 and 984 are located to the northeast

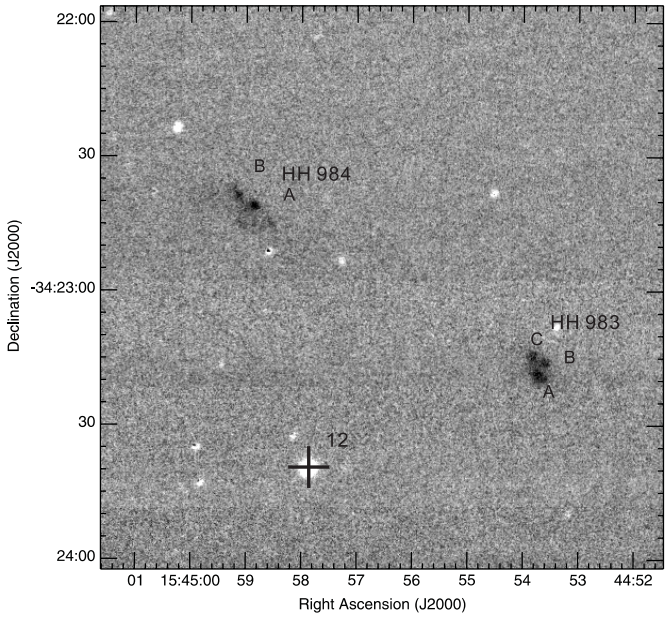

Figure 5. Continuum subtracted [S II] image of HH 983 and 984. YSO 12 from Merín et al. (2008) is marked with plus.

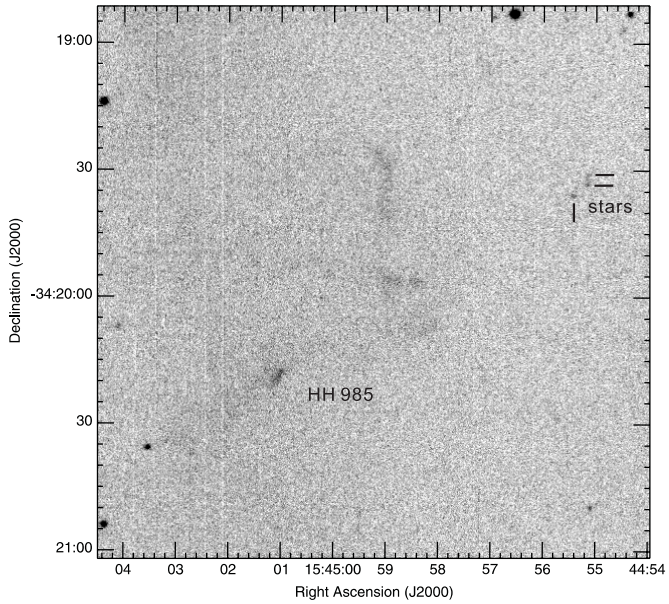

Figure 6. [S II] image of HH 985. For clarity, the three stars on the upper right of the image are indicated.

of HH 981 and 982. HH 983 consists of three emission patches and HH 984 consists of two elongated knots (see Figure 5). The morphology of HH 983 and 984 suggests that they are driven by the PMS star Sz 69, a Class II YSO (YSO 16 in Merín et al. 2008; see Figure 3). HH 985 is a faint feature near the center of Figure 3. For HH 985, due to its faintness, the direct [S II] image, rather than the continuum subtracted one, is given in Figure 6 to avoid the noise introduced by continuum subtraction. In Figure 6, about 30″ to the northwest of HH 985 a faint curved [S II] emission feature of dimension of ∼ 30″ can be seen. On the basis of the overall morphology of HH 985 and the locations of the nearby YSOs in the region (see Figure 3), YSOs 14 and 17 (Merín et al. 2008) are possible driving sources for this HH object. HH 987 is located about 4′ to the east of HH 982. It is an elongated knot with a long tail extending to the northeast (see

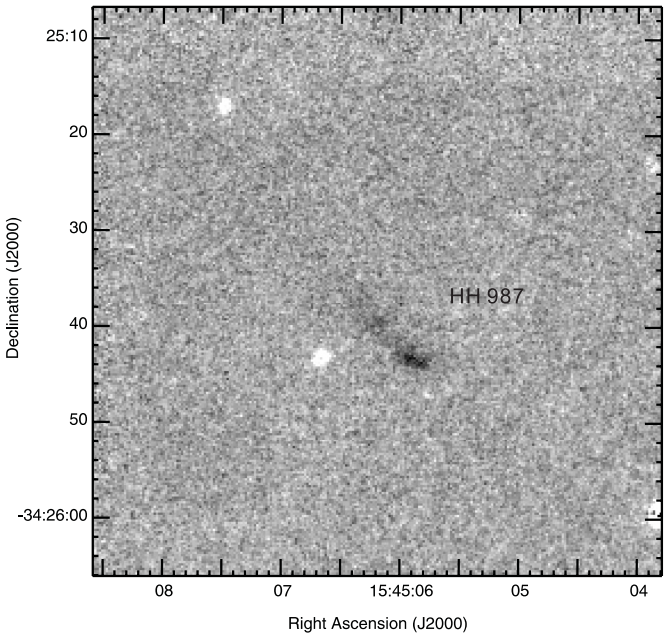

Figure 7. Continuum subtracted [S II] image of HH 987.

Figure 7). As in the case of HH 985, we tentatively propose that HH 987 is driven by YSO 17.

HH 986, a faint knot with a long tail extending to the northeast, is about 90″ to the east of the young star Sz 68, the driving source of the HH 186 jet (see Figure 8). Recently, two YSOs, SSTc2d J154506.3−341738 and J154508.9−341734 (YSOs 13 and 14), were found in this region based on their spectral index in the 2 μm–24 μm wavelength range (Chapman et al. 2007; Merín et al. 2008). YSO 14 has a spectral index of class II, while YSO 13 has a flat spectrum in the 2 μm–24 μm wavelength range (Chapman et al. 2007; Merín et al. 2008). The PMS star Sz 69 is also located in this region. The locations of YSOs in the region are marked with pluses in Figure 8. From Figure 8 it can been seen that the long tail of HH 986 points toward YSO 13. Based on this configuration we propose that HH 986 is driven by YSO 13. Furthermore, in Figure 8 we can see faint arc-like emission extending from the HH 187 knot (Heyer & Graham 1989) to the northwest. This morphology excludes the nearby YSOs, i.e., YSOs 12–17, as the driving source of HH 187 (see Figure 3), and may suggest a driving source located far away to its northwest (see Figure 1).

In combination with other surveys, the *Spitzer* c2d observations revealed a small cluster of young stars in the Sz 68 region which includes YSOs 12-17. The abundance of HH objects detected in this region in our survey confirms that this region is active in star formation, although the Lupus I cloud as a whole is only modest in star formation. As discussed above, as many as seven outflows may exist in this region, i.e., the HH 981 and 982 flow driven by YSO 12, the HH 983 and 984 flow driven by Sz 69, the HH 987 flow and the HH 985 flow, the HH 186 flow driven by Sz 68, the HH 986 flow driven by YSO 13, and the HH 187 flow (see Figure 3). We note that the HH objects in this region as a whole are weak, in terms of emission brightness and physical dimension, as compared to HH objects found in the R CrA and Cha I star-forming regions that are at similar distances as Lupus I and III and have been surveyed with the same techniques (see Wang et al. 2004 and Wang & Henning 2006). This difference can be attributed to the fact that the stellar contents in the Lupus clouds are found to be dominated by late-type stars as compared to other low-mass star forming regions such as the Taurus star-forming clouds (Hughes et al. 1994). The accretion rates of young stars decrease with the mass of central stars in a form of $\dot{M} \sim 10^{-8}\, M_{\odot}\ \mathrm{yr}^{-1}(M/M_{\odot})^2$ (Muzerolle et al. 2003, 2005). Therefore, less massive stars are expected to drive weaker outflows.

HH 988 is an isolated HH object located at the southeastern outskirts of the Lupus I cloud (see Figure 1). It is a faint patch with a dimension of about 10″ in the north–south direction and about 4″ in the east–west direction. The [S II] image of

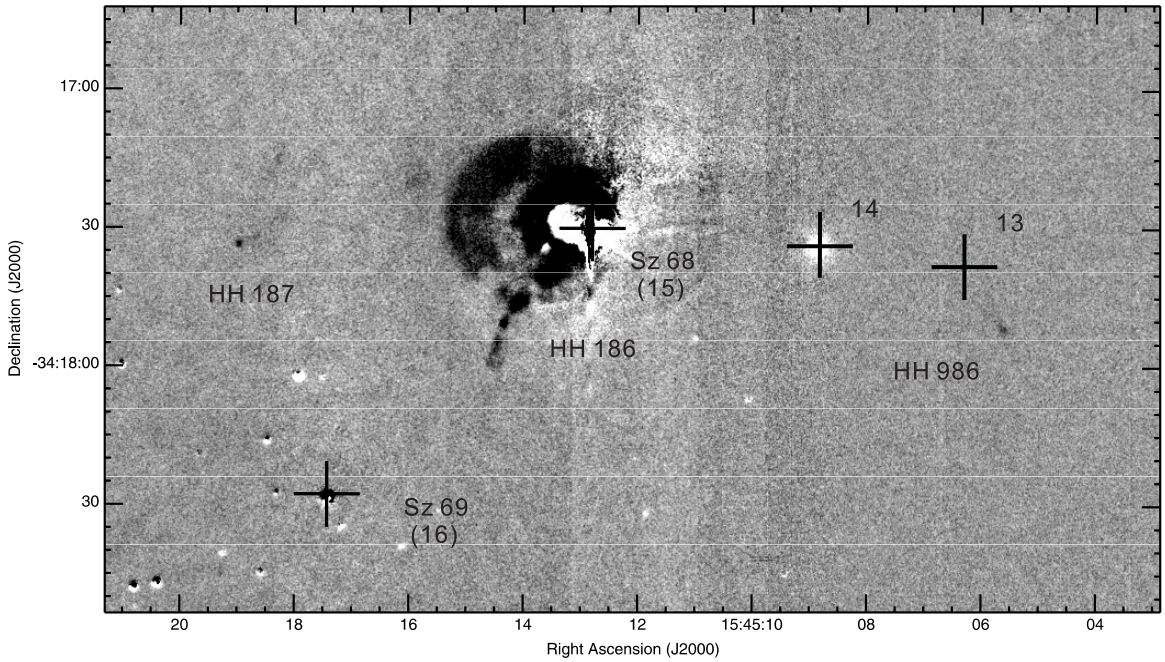

Figure 8. Continuum subtracted [S II] image of the HH 986 region. The previously known HH objects, HH 186 and 187, are indicated. YSOs 13–16 from Merín et al. (2008) are marked with pluses.

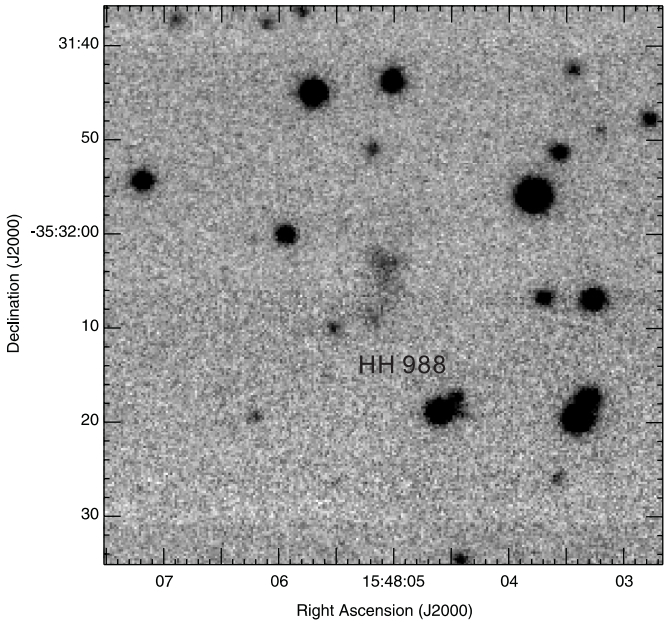

Figure 9. [S II] image of HH 988.

this object is given in Figure 9. No features can be found in the 2MASS JHK images at the position of HH 988. Therefore we can eliminate the possibility that this object is an emission galaxy and we believe that it is an HH object. The T Tauri star HM Lup is located 4.′6 to the northwest of HH 988 and may be the driving source (see Figure 1).

The previously known HH 185 object is located in the Barnard 228 dark cloud in the Lupus I region (see Figure 1). This object has shown substantial change in morphology during the time from 1988 to 2005. In the discovery image of Figure 5 in Heyer & Graham (1989), which was obtained in 1988, HH 185 shows a morphology of elongated patch with two emission peaks oriented in the direction of northeast–southwest. The centroid of the southwestern peak coincides with YSO 10 (IRAS 15398−3359) in Merín et al. (2008). The northeastern peak has a brightness similar to that of the southwestern peak and is located about 5″ to the southwestern peak. In our [S II] image (see Figure 10), however, HH 185 is roughly a round patch with a central concentration that coincides well with YSO 10. The northeastern peak of HH 185 in Figure 5 of Heyer & Graham (1989) disappears entirely in our image that was obtained in 2005.

Using the *Spitzer* IRAC images obtained for the c2d program, Merín et al. (2008) conducted a search for mid-infrared high-velocity outflows and nebulae in the Lupus I, III, and IV clouds. In the Lupus I cloud they only found mid-infrared emission from HH 185−187 and IRAS 15356−3430. IRAS 15356−3430 is outside of our images. In terms of detection rate, our optical survey of high-velocity outflows in the Lupus I cloud is more sensitive than the survey made in the mid-infrared with *Spitzer* IRAC.

3.2. HH Objects in the Lupus III Cloud

In the Lupus III cloud we detected six HH objects including three previously known HH objects, HH 78, 228, and 600 (see Figure 2). All six HH objects are concentrated in the central part of the cloud around the brightest stars in the Lupus III cloud, i.e., the Herbig Ae/Be stars HR 5999 and HR 6000 (see Figures 2 and 11). The detection of these HH objects together with the presence of plenty of YSO sources in this region indicates that active star formation is taking place in this part of the Lupus III cloud.

HH 228 consists of a short jet emanating from the driving source, Th 28, and the emission objects HH 228 E and W which were reported to be 30″ east and 38″ west of Th 28, respectively (Krautter 1986). Graham & Heyer (1988) detected an additional emission feature, HH 228 E2, which was reported to be 87″ southeast of the driving star and located exactly on the line defined by the HH 228 jet and HH 228 E and W. Our continuum subtracted [S II] image of this region is presented in Figure 12. From this image the separations of HH 228 E2, E, and W from the driving star are measured to be 95″, 39″, and 45″, respectively. Our measurements differ from previously reported values by 8″, 9″, and 7″, respectively. The observations by Krautter (1986) were made on 1985 May 27–29 and those by Graham & Heyer (1988) were on 1988 June 4. With a temporal baseline of 16.1 yr for HH 228 E2 and 19.1 yr for HH 228 E and W, the proper motions for HH 228 E2, E, and W are calculated to be 0.″50 yr^{-1}, 0.″47 yr^{-1}, and 0.″37 yr^{-1}, respectively. Our proper motion measurement for HH 228 E is very close to the value of 0.″5 yr^{-1} reported by Krautter (1986). Taking a distance of 150 pc for this region, the tangential velocities for HH 228 E2, E, and W are estimated to be 357 km s^{-1}, 335 km s^{-1}, and 264 km s^{-1}, respectively. The dynamical ages for HH 228 E2, E, and W as determined from their proper motions are only 190, 83, and 122 yr, respectively. If each of these emission features represents a burst of mass outflow from the driving source Th 28, we can see that the period of mass outflow burst of the protostar Th 28 is as short as ∼50 yr.

HH 989 is a faint emission patch about 6′ to the east of the HH 228 jet (see Figures 11 and 13). In its environment there are several YSOs (Merín et al. 2008; see Figure 11). Its driving

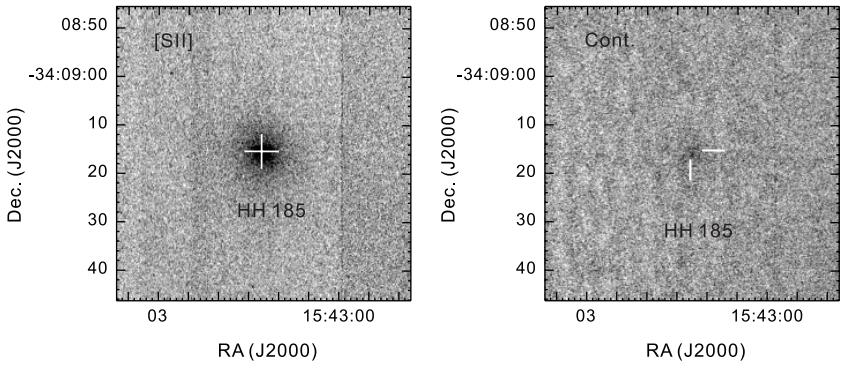

Figure 10. [S II] (left) and continuum (right) images of HH 185. The position of YSO 10 (IRAS 15398−3359) from Merín et al. (2008) is indicated in both images.

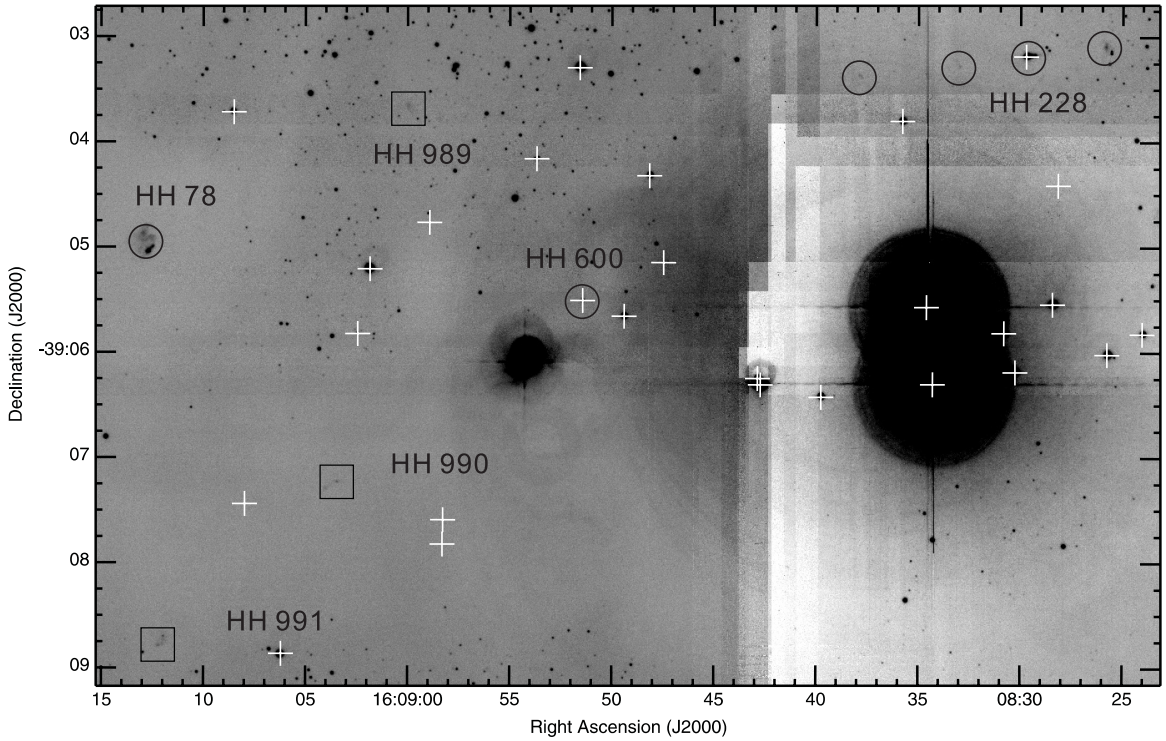

Figure 11. [S II] image of the central part of Lupus III. The newly found HH objects, HH 989-991, are indicated with squares. The previously know HH objects, HH 228, 228 W, 228 E, 228 E2, 600, and 78, are indicated with circles. The locations of YSOs from Merín et al. (2008) are marked with white pluses. The two bright stars on the right side of the image are the Herbig Ae/Be stars HR 5999 and HR 6000.

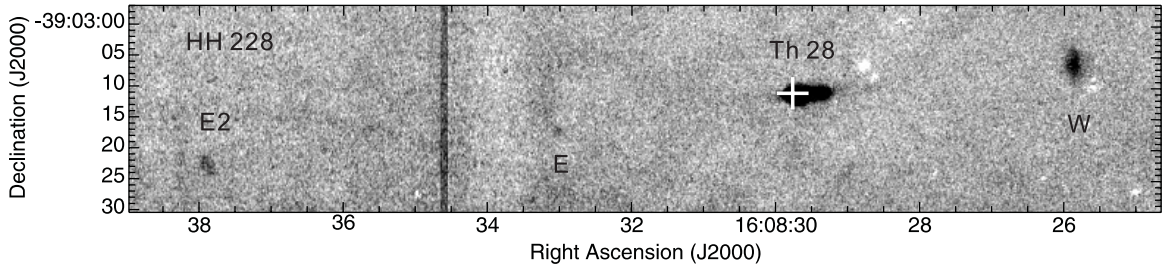

Figure 12. Continuum subtracted [S II] image of the HH 228 region.

source is unclear. It is possible that HH 989 is an extension to the highly collimated HH 228 flow on the basis that it is exactly located on the axis of the flow.

HH 600 is a short jet emanating from the very low-mass star Par-Lup3-4. This jet was discovered by Fernández & Comerón (2005). The continuum subtracted [S II] image of HH 600 is presented in Figure 14. HH 990 is about 3′ to the southeast of the HH 600 jet (Figure 11). It consists of knot A and patch B (Figure 15). These components are oriented in the northwest–southeast direction. HH 991 is located about 140″ to the southeast of HH 990 (Figure 11). This object has a comma-like shape. Its [S II] image is presented in Figure 16. We note that HH 600 and HH 990–991 are well aligned in the direction of P.A. $\sim 130^{\circ}$, very close to the orientation of the HH 600 jet which was measured to be P.A. $= 129\overset{\circ}{.}7$ (Fernández & Comerón 2005). These facts suggest that HH 990 and 991 are probably part of the flow driven by Par-Lup3-4, a very low-mass star of spectral type of M5 (Comerón et al. 2003). The separation from HH 991 to Par-Lup3-4 is 312″, corresponding to a linear length of 0.23 pc at a distance of 150 pc to Lupus III. Assuming a tangential velocity of 150 km s^{-1} for HH 991, the dynamical age of HH 991 is 1.5×10^3 yr if this object is driven by the very low-mass star Par-Lup3-4. We note that no counterpart flow can be found to the NW of Par-Lup3-4 in our image.

Our high resolution continuum subtracted [S II] image of the previously known object HH 78 is presented in Figure 17. Graham & Heyer (1988) suggested that HH 78 may be powered by Th 28 on the basis that it is located near the axis of the HH 228 flow. By comparing the coordinates of HH 78 reported by Reipurth & Graham (1988) and those obtained from our image (see Table 2), however, we find that HH 78 exhibits nearly no measurable proper motion between the two observing epochs which have a time span of 18 yr. As HH 228 E2, E, and W all exhibit substantial proper motions, we conclude that HH 78 is unlikely to be powered by the exciting source of the HH 228 flow, i.e., Th 28. The Class I source in Merín et al. (2008), Lupus 3 MMS (YSO 87), is located 64″ to the east of HH 78. Tachihara et al. (2007) detected blueshifted high-velocity wings in their CO ($J = 3$–2) line observations toward Lupus 3 MMS which imply a molecular outflow coming from this MMS and they suggested that HH 78 results from this outflow.

The median of the peak brightness of the 17 HH objects observed in Lupus I and III is about nine times that of our detection limit (3σ). The brightest HH object in this region is

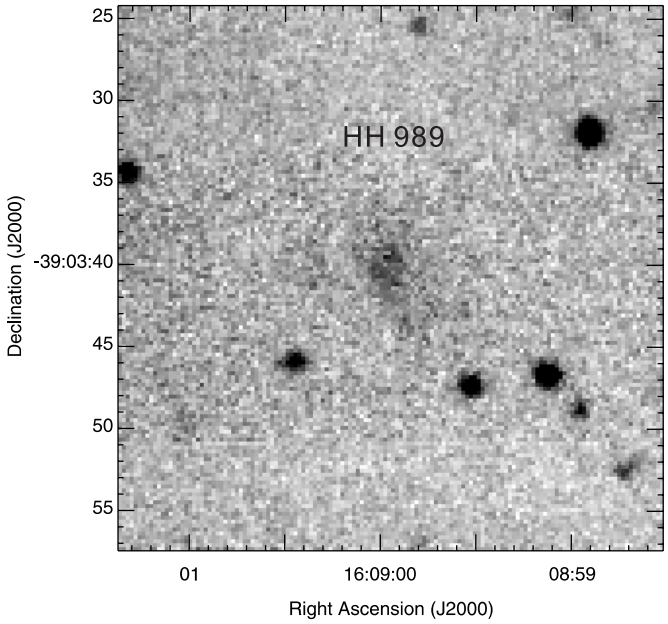

Figure 13. [S II] image of HH 989.

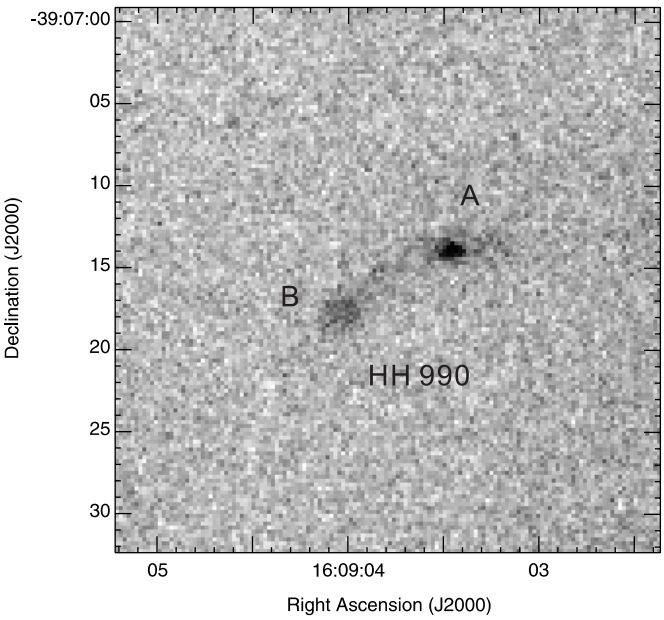

Figure 15. Continuum subtracted [S II] image of HH 990.

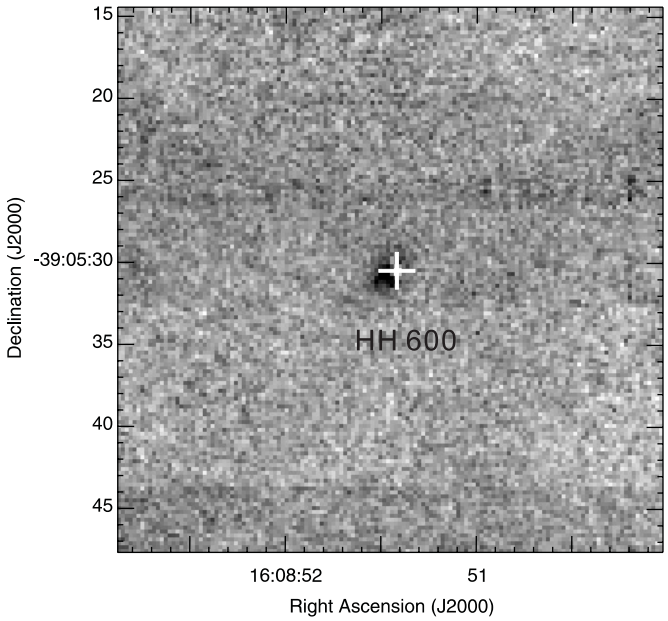

Figure 14. Continuum subtracted [S II] image of HH 600. The position of Par-Lup3-4, a low-mass star of spectral type M5, is marked with a white plus.

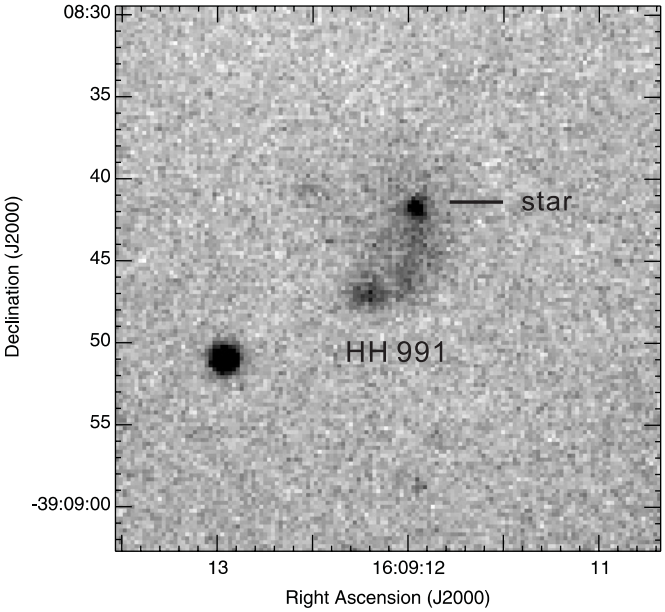

Figure 16. [S II] image of HH 991.

HH 78, the peak brightness of which is about 50 times that of our detection limit. Taking the median peak brightness of the 17 HH objects as a typical value for the peak brightness of all HH objects located in the Lupus I and III clouds, and assuming that the average extinction of the 17 HH objects observed in our survey is 1 mag at R band, we estimated that our observations can detect HH objects up to a cloud depth of $A_R = 3.4$ mag ($A_V = 4.5$ mag). For HH objects as bright as HH 78, our observations can detect them up to a cloud depth of $A_R = 5.3$ mag ($A_V = 7.1$ mag).

Merín et al. (2008) found mid-infrared emission from HH 228 E and W, HH 78, Lupus 3 MMS, and a jet located at $\alpha = 16^{\rm h}10^{\rm m}57\overset{\rm s}{.}95$, $\delta = -38^{\circ}04'37\overset{''}{.}90$ (J2000) in the Lupus III cloud. The mid-infrared jet is outside of our optical images. The mid-infrared outflow from Lupus 3 MMS is the only outflow in the Lupus I and III clouds that is observed with *Spitzer* IRAC but not detected in our optical survey. As in the case of Lupus I, we can see that our optical survey of high-velocity outflows is more sensitive, in terms of detection rate, than the survey made with Spitzer IRAC in the c2d program. From the downloaded Spitzer c2d images we estimated that the c2d detection limit in IRAC band 2 is around 1.9×10^{-19} W m^{-2} arcsec^{-2} (3σ). As little information about the typical brightness of mid-infrared outflows is currently available in the literature, we used the synthetic Spitzer IRAC band maps of Smith & Rosen (2005) to estimate the brightness of mid-infrared outflows and compare it with the Spitzer IRAC detection limit. In the numerical simulations of Smith & Rosen (2005), the typical integrated H_2 luminosities in IRAC band 2 is around 2.0×10^{30} erg s^{-1} (see their Table 3), which corresponds to a brightness of 2.4×10^{-18} W m^{-2} arcsec^{-2} assuming a physical dimension of

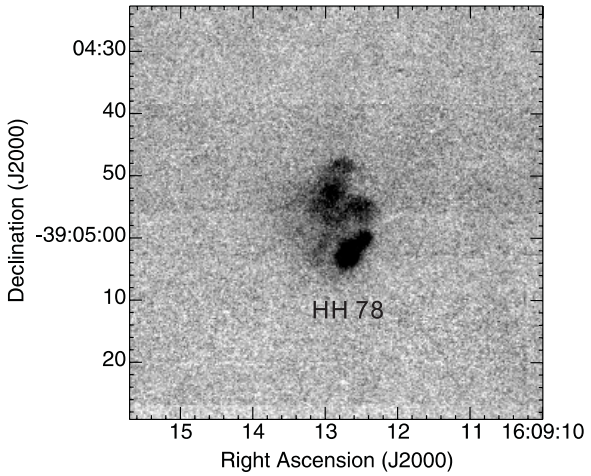

Figure 17. Continuum subtracted [S II] image of HH 78.

4×10^{16} cm for the outflows (see their Figure 8). Therefore, the ratio of typical brightness to detection limit for IRAC band 2 observations of mid-infrared outflows is estimated to be around 12, a little bit larger than the ratio estimated for our optical survey of HH objects. The excitation of H_2 mid-infrared emission in outflows from YSOs requires the presence of dense molecular gas in the surrounding of the high-velocity jets. In the models of Smith & Rosen (2005), the ambient gas surrounding the high-velocity jets is assumed to have a density of 10^4 cm^{-3}. The lower detection rate of outflows in the Spitzer c2d survey than in our optical survey may indicate that no or little dense molecular gas exists in the surrounding of most outflows in the Lupus I and III clouds. Therefore, except for outflows deeply embedded in dense molecular gas, optical surveys appears to be more sensitive than mid-infrared surveys to high-velocity outflows.

Through near-infrared imaging (Nakajima et al. 2000), deep slitless spectroscopy (Comerón et al. 2003), optical imaging (López Martí et al. 2005), and Spitzer IRAC and MIPS photometry (Allers et al. 2006; Allen et al. 2007), 19 young brown dwarfs or brown dwarf candidates have been identified in the Lupus I and III clouds, among which 15 young brown dwarfs or brown dwarf candidates are located within our survey area. Except for the young brown dwarf SSTc2d J154457.9−342340 that probably drives HH 981 and 982 (see discussion in Section 3.1), no evidence for other young brown dwarfs to drive HH objects has been found in our survey. The low detection rate of optical outflows from young brown dwarfs in our survey is not a surprise if we consider that the mass-loss rates of young brown dwarfs are 2 orders of magnitude lower than the mass-loss rates of T Tauri stars. Masciadri & Raga (2004) estimated that the H_α luminosity of a jet from a brown dwarf embedded in a neutral region will be 2 orders of magnitude lower than that of a typical jet from a typical T Tauri star.

4. SUMMARY

We performed a deep search for HH objects toward the Lupus I and III clouds covering a sky area of ~ 1 and ~ 0.5 deg^2, respectively. The results are summarized in the following:

1. In total, 11 new HH objects, HH 981–991, are discovered. HH objects both in Lupus I and Lupus III are concentrated in small regions. The HH objects detected in Lupus I are clustered in a region of radius 0.26 pc near the young star Sz 68. The abundance of HH objects in this region shows that this part of the Lupus I cloud is active in ongoing star formation which is also revealed by the presence of a small cluster of YSOs in this region. The HH objects detected in Lupus III are concentrated in the central part of the cloud around HR 5999 and HR 6000. HH 981 and 982 in Lupus I are probably driven by the young brown dwarf SSTc2d J154457.9−342340 which has a mass of 50 M_J. HH 990 and 991, with a separation of 0.13 pc and 0.23 pc from Par-Lup3-4, are probably excited by this very low-mass star of spectral type M5.
2. High proper motions for HH 228 E2, E, and W are measured, which confirms that they are excited by the young star Th 28. In contrast, HH 78 exhibits no measurable proper motion, suggesting that HH 78 is not part of the HH 228 flow, although HH 78 is located on the axis of the flow.
3. In addition to the new HH objects, our optical survey recovers all outflows detected in the Spitzer c2d survey except for the mid-infrared outflow from Lup3 MMS. Therefore, it can been concluded that our optical survey is in general more sensitive to high-velocity outflows than the Spitzer c2d survey.

We thank the ESO/MPG 2.2m WFI group for making the observations in service mode. We thank the anonymous referee for his/her useful comments that helped improve the manuscript. This paper is part of an ongoing collaboration between the Purple Mountain Observatory in Nanjing and the Max Planck Institute for Astronomy in Heidelberg. H.W. acknowledges the support by NSFC grants 10733030 and 10621303.

REFERENCES

Allen, P. R., Luhman, K. L., Myers, P. C., Megeath, S. T., Allen, L. E., Hartmann, L., & Fazio, G. G. 2007, ApJ, 655, 1095
Allers, K. N., Kessler-Silacci, J. E., Cieza, L. A., & Jaffe, D. T. 2006, ApJ, 644, 364
Arce, H. G., Shepherd, D., Gueth, F., Lee, C.-F., Bachiller, R., Rosen, A., & Beuther, H. 2007, in Protostars and Planets V (Tucson, AZ: Univ. Arizona Press), 245
Baade, M. 2002, Wide Field Imager (WFI) User Manual, http://www.ls.eso.org/lasilla/Telescopes/2p2T/E2p2M/WFI/docs/manual/wfiuserman-1.0.7.ps
Bachiller, R. 1996, ARA&A, 34, 111
Bally, J., Reipurth, B., & Davis, C. J. 2007, in Protostars & Planets V, ed. B. Reipurth, D. Jewitt, & K. Keil (Tucson, AZ: Univ. Arizona Press), 215
Barrado y Navascués, D., Mohanty, S., & Jayawardhana, R. 2004, ApJ, 604, 284
Chapman, N. L., et al. 2007, ApJ, 667, 288
Comerón, F. 2008, in Handbook of Star Forming Regions: Vol. II. The Southern Sky, ed. B. Reipurth (San Francisco, CA: ASP), 295
Comerón, F., Fernández, M., Baraffe, I., Neuhäuser, R., & Kaas, A. A. 2003, A&A, 406, 1001
Fernández, M., & Comerón, F. 2001, A&A, 380, 264
Fernández, M., & Comerón, F. 2005, A&A, 440, 1119
Fesen, R. A., & Hurford, A. P. 1996, ApJS, 106, 563
Graham, J. A., & Heyer, M. H. 1988, PASP, 100, 1529
Hara, A., Tachihara, K., Mizuno, A., Onishi, T., Kawamura, A., Obayashi, A., & Fukui, Y. 1999, PASJ, 51, 895
Hartigan, P., Morse, J. A., Tumlinson, J., Raymond, J., & Heathcote, S. 1999, ApJ, 512, 901
Herbig, G. H., & Bell, K. R. 1988, Lick Obs. Bull. 1111
Heyer, M. H., & Graham, J. A. 1989, PASP, 101, 816
Hughes, J., Hartigan, P., Krautter, J., & Kelemen, J. 1994, AJ, 108, 107
Knude, J, & Høg, E. 1998, A&A, 338, 897
Krautter, J. 1986, A&A, 161, 195

Krautter, J. 1991, in Low Mass Star Formation in Southern Molecular Clouds, ed. B. Reipurth (Garching: ESO), 127
Kwitter, K. B., & Henry, R. B. C. 1998, ApJ, 493, 247
Lombardi, M., Lada, C. J., & Alves, J. 2008, A&A, 480, 785
López Martí, B., Eislöffel, J., & Mundt, R. 2005, A&A, 440, 139
Masciadri, E., & Raga, A. C. 2004, ApJ, 615, 850
Merín, B., et al. 2008, ApJS, 177, 551
Muzerolle, J., Hillenbrand, L., Calvet, N., Briceño, C., & Hartmann, L. 2003, ApJ, 592, 266
Muzerolle, J., Luhman, K. L., Briceño, C., Hartmann, L., & Calvet, N. 2005, ApJ, 625, 906
Nakajima, Y., Tamura, M., Oasa, Y., & Nakajima, T. 2000, AJ, 119, 873
Natta, A., Testi, L., Muzerolle, J., Randich, S., Comerón, F., & Persi, P. 2004, A&A, 424, 603
Osterbrock, D. E., Tran, H. D., & Veilleux, S. 1992, ApJ, 389, 305
Pudritz, R. E., Ouyed, R., Fendt, C., & Brandenburg, A. 2007, in Protostars and Planets V, ed. B. Reipurth, D. Jewitt, & K. Keil (Tucson, AZ: Univ. Arizona Press), 277
Reipurth, B., & Bally, J. 2001, ARA&A, 39, 403
Reipurth, B., & Graham, J. A. 1988, A&A, 202, 219
Schwartz, R. D. 1977, ApJS, 35, 161
Shang, H., Li, Z.-Y., & Hirano, N. 2007, in Protostars and Planets V, ed. B. Reipurth, D. Jewitt, & K. Keil (Tucson, AZ: Univ. Arizona Press), 261
Smith, M. D., & Rosen, A. 2005, MNRAS, 357, 1370
Solf, J., Böhm, K. H., & Raga, A. 1988, ApJ, 334, 229
Tachihara, K., Dobashi, K., Mizuno, A., Ogawa, H., & Fukui, Y. 1996, PASJ, 48, 489
Tachihara, K., Toyoda, S., Onishi, T., Mizuno, A., Fukui, Y., & Neuhäuser, R. 2001, PASJ, 53, 1081
Tachihara, K., et al. 2007, ApJ, 659, 1382
Walawender, J., Bally, J., & Reipurth, B. 2005, AJ, 129, 2308
Wang, H., & Henning, Th. 2006, ApJ, 643, 985
Wang, H., Mundt, R., Henning, Th., & Apai, D. 2004, ApJ, 617, 1191
Whelan, E. T., Ray, T. P., Bacciotti, F., Natta, A., Testi, L., & Randich, S. 2005, Nature, 435, 652
Whitworth, A., Bate, M. R., Nordlund, Å., Reipurth, B., & Zinnecker, H. 2007, in Protostars and Planets V, ed. B. Reipurth, D. Jewitt, & K. Keil (Tucson, AZ: Univ. Arizona Press), 459
Wichmann, R., Bastian, U., Krautter, J., Jankovics, I., & Rucinski, S. M. 1998, MNRAS, 301L, 39
Yan, J., Wang, H., Wang, M., Deng, L., Yang, J., & Chen, J. 1998, AJ, 116, 2438